Robust Control of Mechatronic Systems
Lab 2: Clutch and Anti-roll Control

Students: TIRACH Raquel, SCHILD Lukas, and TRAN Gia Quoc Bao

Date: 25 January 2021

1 Introduction

During this lab, we apply what we have studied in robust control to the problem of clutch and anti-roll control of a vehicle. We first design and then tune an $\mathcal{H}_\infty$ controller so that it meets all the predefined requirements, then verify that this controller is robust against unstructured uncertainties. For the second part, we improve the driver's and passengers' comfort regarding the car's suspension by designing appropriate weighting functions used in an $\mathcal{H}_\infty$ controller.

2 $\mathcal{H}_\infty$ control of a clutch flexible system

In this section, we consider the drive train dynamics. The system under consideration consists of an actuator connected to a load through a torsional spring, which represents the joint flexibility. The equations of motion are derived using the generalized coordinates θ_l and θ_m, respectively the link (load) angle and the motor angle, and the input u, the motor torque.

$$\begin{cases} J_l\ddot{\theta}_l + B_l\dot{\theta}_l + k(\theta_l - \theta_m) = 0 \\ J_m\ddot{\theta}_m + B_m\dot{\theta}_m - k(\theta_l - \theta_m) = u \end{cases} \tag{1}$$

where J_l and J_m are the load and motor inertia, B_l and B_m are the load and motor damping constants, with $k = 0.8NM/rad$, $J_m = 4.10^4 NMs^2/rad$, $J_l = 4.10^4 NMs^2/rad$, $B_m = 0.015NMs/rad$, $B_l = 0NMs/rad$. The controlled output is the load angle θ_l. The open loop transfer function from the control input u to θ_l is:

$$\frac{\theta_l}{u} = \frac{k}{p_l(s)p_m(s) - k^2} \tag{2}$$

where $p_l(s) = J_l s^2 + B_l s + k$ and $p_m(s) = J_m s^2 + B_m s + k$.

In this study, the aim is to design an $\mathcal{H}_\infty$ controller such that the closed-loop system satisfies all the following performance specifications:

- Robustness: Module margin > 0.5
- Settling time $< 0.5s$, tracking steady state error $< \frac{1}{1000}$.
- Attenuation of input disturbance step, with "no" steady-state error. This type of disturbance is some load torque on the input u.
- Sensitivity of the control input to sinusoidal measurement noise at $800rad/s < 10\%$.
- Actuator constraint: Maximal controller gain = 3.

2.1 Performance analysis and specifications

A proportional-derivative (PD) control with load angle feedback is given as :

$$K(s) = K_d s + K_p \tag{3}$$

where $K_d = 0.0033$ and $K_p = 0.3$.

First of all, we analyze this PD controller in terms of stability and performance and verify if the performance specifications are met, by plotting the four sensitivity functions.

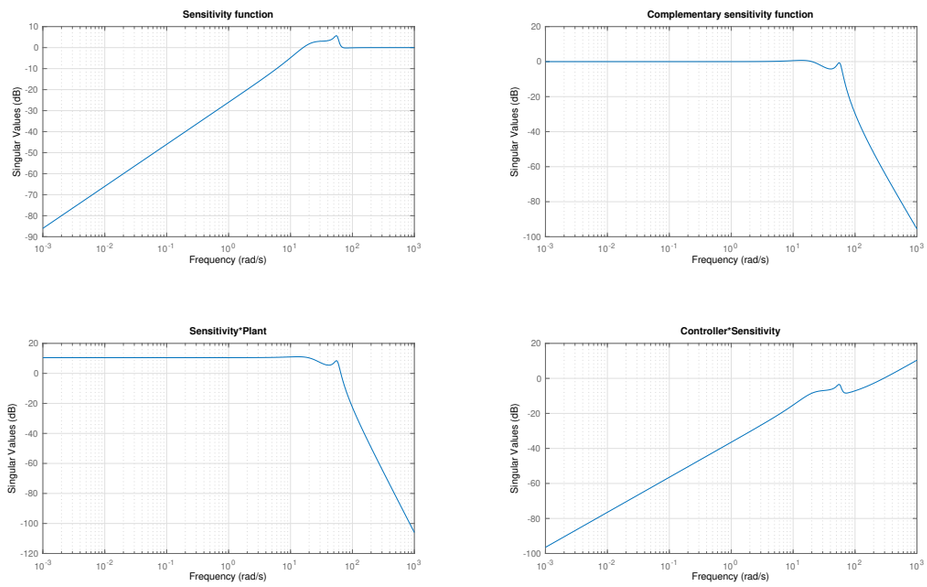

Figure 1: Sensitivity functions for a PD controller

- The closed-loop system is internally stable since the real parts of the poles of all the sensitivity functions are negative.
- The system is robust since $M_S \approx 5.6dB < 6dB$ which implies that $\Delta M > 0.5$. Additionally, $M_T \approx 1.1dB < 3.5dB$.
- We have $\epsilon_r = |S(\omega = 0)| < 10^{-4}$ which means that the steady state tracking error is $< \frac{1}{1000}$, satisfying the requirement.
- The complementary sensitivity function T shows us that $\omega_T \approx 31.4rad/s$ which implies that $t_r \approx 0.07s < 0.5s$. This is the rise time, but since it is much smaller than $0.5s$, we can say that the settling time meets the requirement.
- With the plant sensitivity function, one can see that $\epsilon \approx 10^{-4}$ at high frequencies. However, input disturbances generally have low frequencies, and at low frequencies, $|SG(j\omega)|$ is large; therefore, this requirement is not met.
- The controller sensitivity function is at $8.5dB$ at $800rad/s$, so the noise attenuation lower than 10% (or $-20dB$) is not achieved by this controller. Additionally, the maximum of the controller sensitivity function is at around $9.5dB$, which is 3, so this requirement is met.

This performance analysis has shown us that the PD controller does not satisfy the required specifications for this system. Therefore, we try using $\mathcal{H}_\infty$ by first designing templates for the sensitivity functions according to the performance specifications. This approach is more intuitive as the requirements are embedded in the templates to shape the desired frequency response.

Template on S

$$\frac{1}{W_e(s)} = \frac{s + \omega_b \epsilon}{s/M_s + \omega_b}$$

In order to meet the specifications, first we design the template such that $\epsilon = 0.001$, $\omega_b = 5rad/s$ and $M_s = 2$.

Template on KS

$$\frac{1}{W_u(s)} = \frac{\epsilon_1 s + \omega_{bc}}{s + \omega_{bc}/M_u}$$

In order to meet the specifications, first we design the template such that $\epsilon_1 = 0.01$, $\omega_{bc} = 80rad/s$ and $M_u = 1.4(\approx 2.92dB)$.

2.2 $\mathcal{H}_\infty$ control

In this part, an $\mathcal{H}_\infty$ control is designed and tuned to solve the problem.

2.2.1 Frequency-domain performance specifications

The adequate control scheme to solve the problem is as follows, where we apply the templates to the tracking error and the control input:

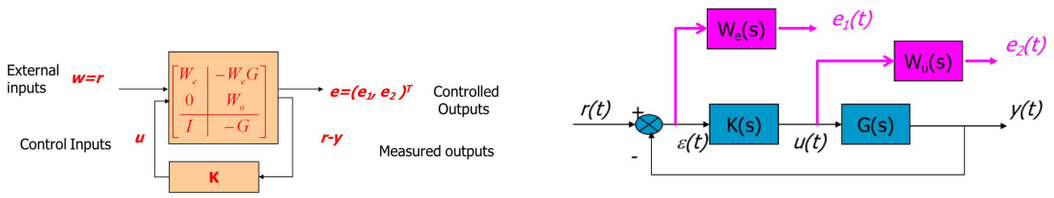

Figure 2: General control configuration

```
% Generalized plant P is found with the sysic function
systemnames = 'G We Wu Wd';
inputvar = '[r(1); d; n; u(1)]';
outputvar = '[We; Wu; r-G-n]';
input_to_G = '[u+Wd]';
input_to_We = '[r-G-n]';
input_to_Wu = '[u]';
input_to_Wd = '[d]';
sysoutname = 'P1';
cleanupsysic = 'yes';
sysic;
```

2.2.2 Design

Test one: Weight on the tracking error only
In this test, we only use the W_e weight in the control configuration.

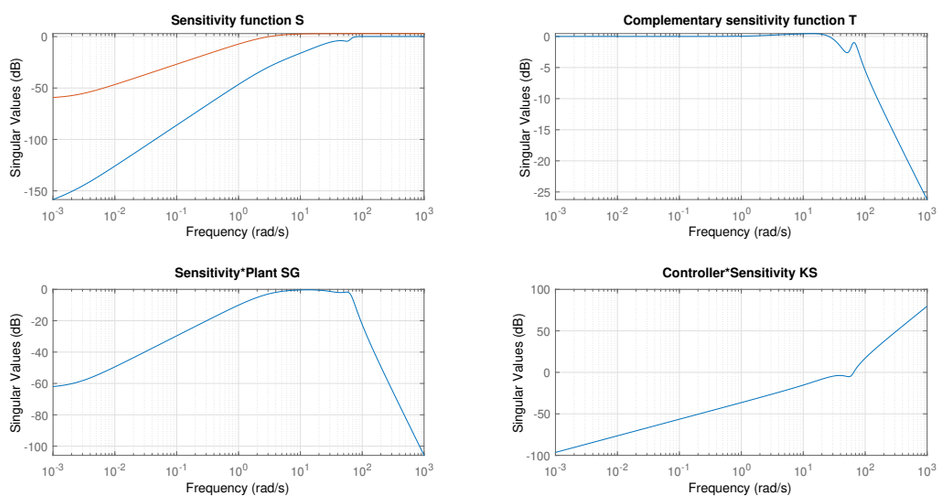

Figure 3: Sensitivity functions for test one

As can be seen in Figure 3, this first test shows that ω_b has to be reduced since the rise time is too fast ($\approx 0.15s$ while we only require $< 0.5s$).

Test two: Weight on the tracking error and the control input
In this test, we use both the W_e and W_u weights in the control configuration.

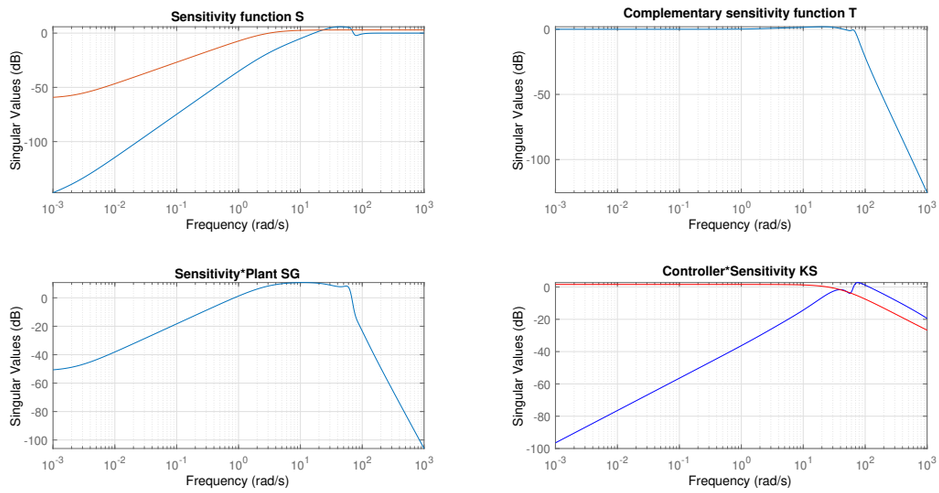

Figure 4: Sensitivity functions for test two

As shown in Figure 4, KS is too big compared to the controller's desired behavior, and the sensitivity of the control input to sinusoidal measurement noise at $800rad/s$ is not lower than $-20dB$ (we have zoomed in to see). We therefore have to reduce ω_{bc} and M_u.

Test three: An additional filter on the noise input
In this test, we use the W_e and W_u weights, as well as W_n in the control configuration.

$$W_n(s) = \frac{3s + 150}{s + 2000} \tag{4}$$

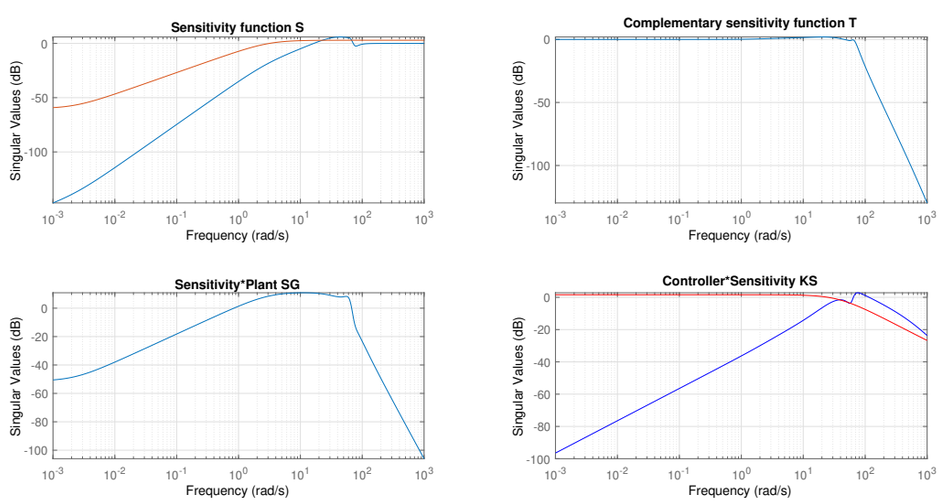

Figure 5: Sensitivity functions for test three

As can be seen in Figure 5, this third test shows a satisfactory attenuation of input disturbance, with "no" steady state error. Also, the sensitivity of the control input to measurement noise at $800rad/s$ is now lower than 10%.
These tests have enabled us to propose a better controller. The template parameters have been changed to:
$\epsilon = 0.001$, $\omega_b = 2.2rad/s$ and $M_s = 1.4$.
$\epsilon_1 = 0.01$, $\omega_{bc} = 45rad/s$ and $M_u = 1.2$.
This new controller meets all the specifications, in particular the ones not met previously: The controller sensitivity function is below $-20dB$ at $800rad/s$ and $|SG(j\omega)|$ is attenuated at low frequencies. Figure 6 shows the sensitivity functions for the best version of the $\mathcal{H}_\infty$ controller.

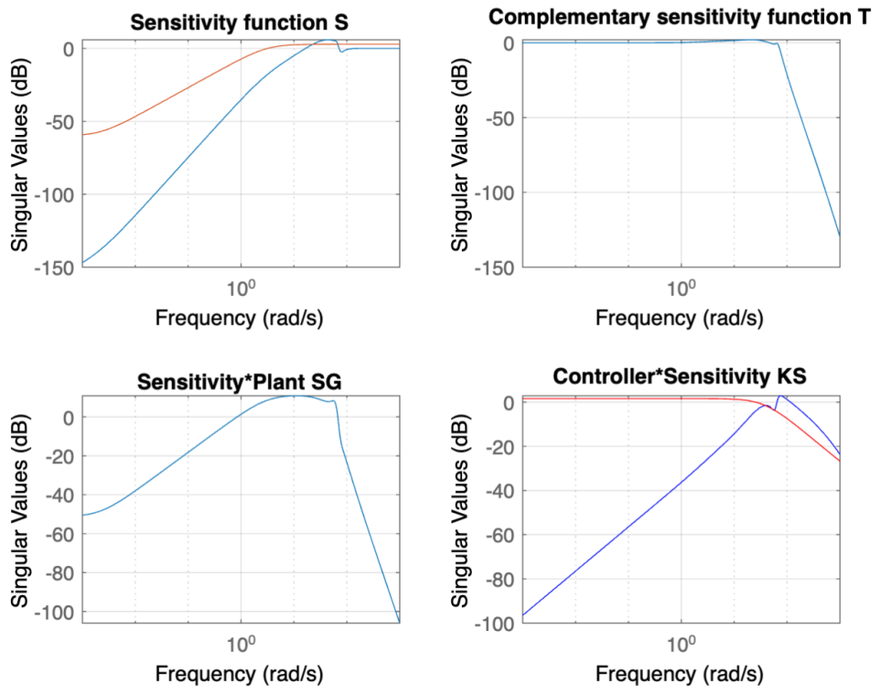

Figure 6: Sensitivity functions for the final controller

2.2.3 Validation using simulation

Now that a better controller has been chosen, it is validated through simulation on **Simulink** in different scenarios.
Figure 7 gives the simulation scheme which has been used in order to validate the controller and to compare it with the previous PD controller. Note that we implement control saturation of $[-1, 1]$ just to test. We perform simulations with both random and sinusoidal measurement noise at $800 rad/s$.

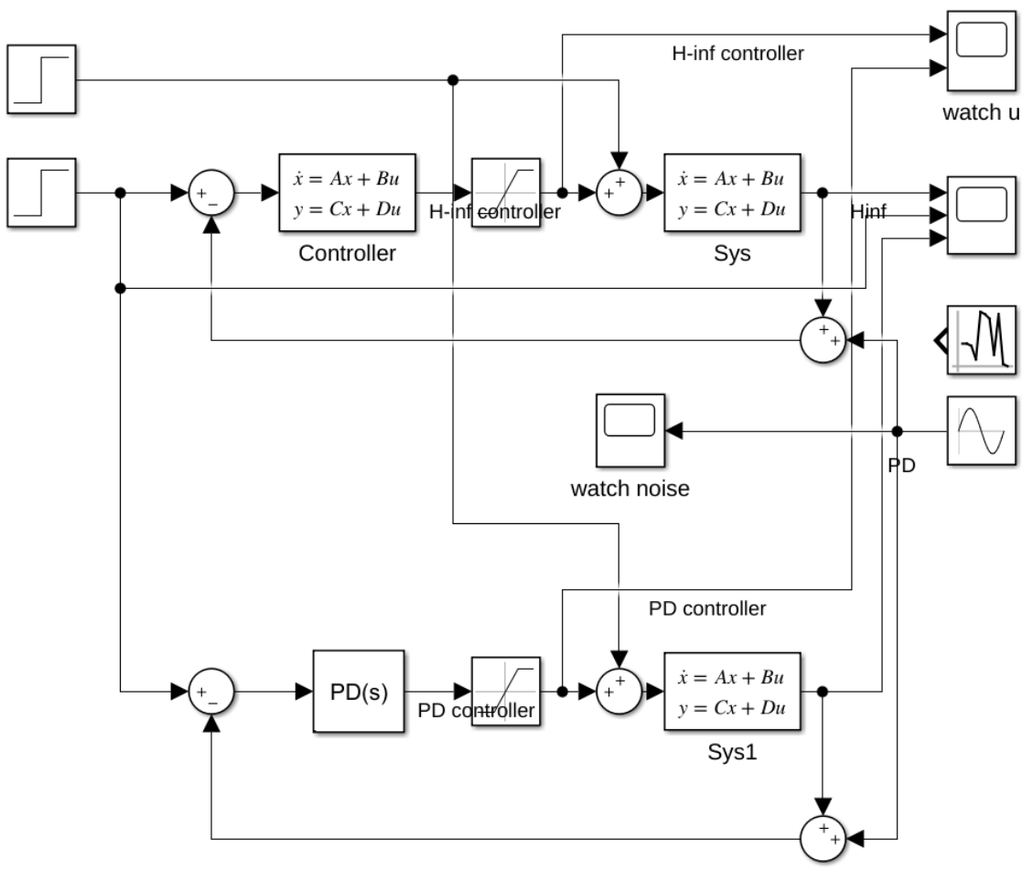

Figure 7: Simulink validation model

Test with random measurement noise

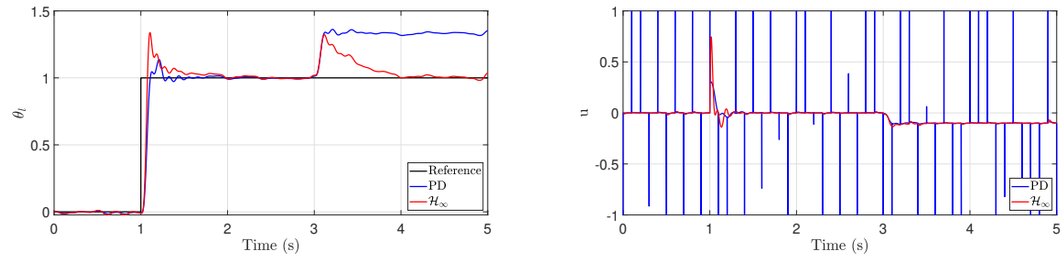

Figure 8: Output (left) and control input (right), with random noise.

Test with sinusoidal measurement noise at $800rad/s$

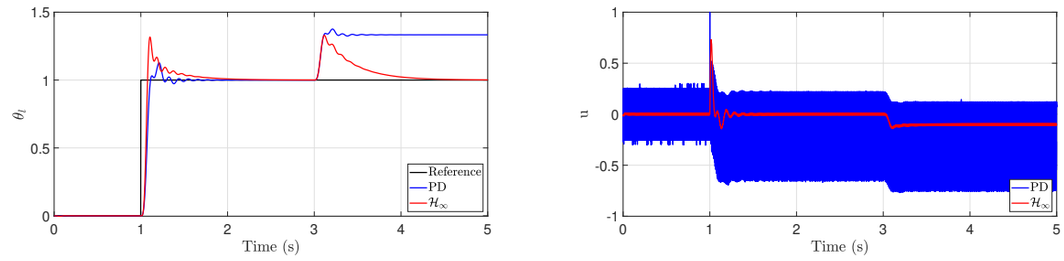

Figure 9: Output (left) and control input (right), with sinusoidal noise at $800rad/s$.

Thanks to the tests, we can see that the $\mathcal{H}_\infty$ controller gives a settling time lower than $0.5s$ and low sensitivity to sinusoidal measurement noise at $800rad/s$ and an ability to reject input disturbances. The $\mathcal{H}_\infty$ controller has a state-space structure where the input is the error, and the output is the control signal. Therefore it has the structure of a PI controller and thus can reject input disturbances.
While the PD controller struggles with both sinusoidal and random number disturbances (see the control input), it is a bit faster than the $\mathcal{H}_\infty$ controller but is unable to reject input disturbances due to the lack of integral action.

2.2.4 Robustness study

Robustness margins
We have $M_S = \max(S) = 5.95dB$ which is smaller than $6dB$, so $\Delta M > 0.5$. Additionally, $M_T = \max(T) = 1.96dB$ which is smaller than $3.5dB$. We can conclude that this $\mathcal{H}_\infty$ controller has satisfactory robustness.

Unstructured uncertainties
We consider now that the system parameters may vary by 10%. Figure 10 shows the difference between the nominal and 25 samples of the uncertain system in the frequency domain.

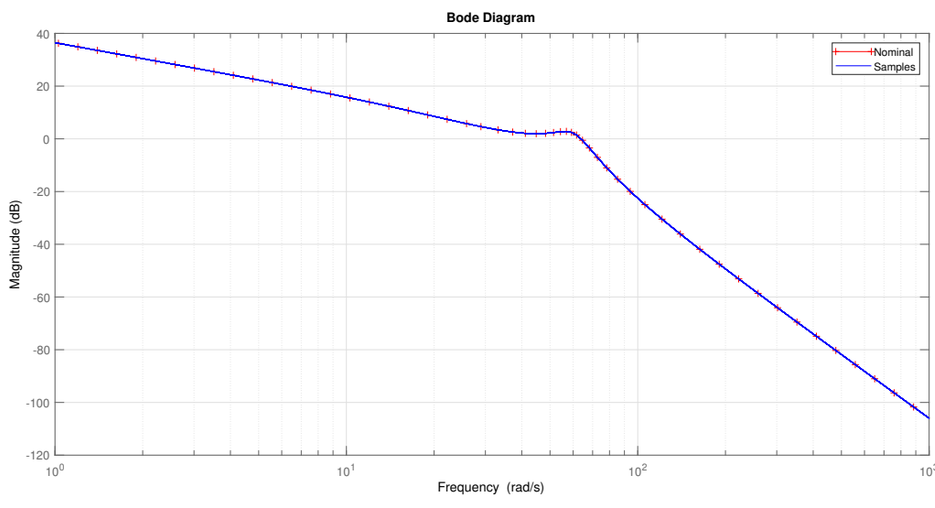

Figure 10: Bode plot of the nominal system and 25 samples of the uncertain system

We then evaluate the relative error between the plant and nominal model to get a frequency-domain representation of multiplicative unstructured uncertainties among orders one, two, and four. This is done using the `ucover` function in MATLAB, which solves an optimization problem. The `ucover` has to be run several times since it is a learning algorithm, and the result depends greatly on the initial values.

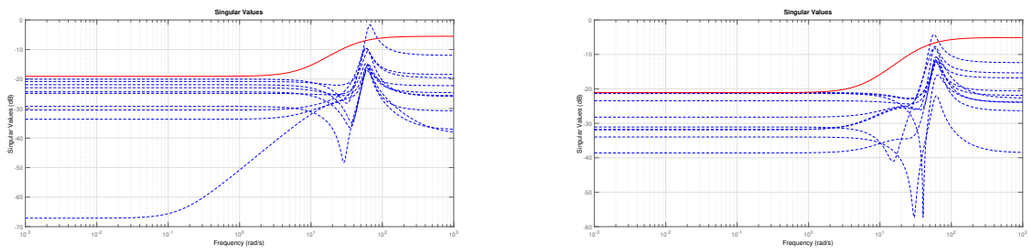

Figure 11: Order one, run one (left) and two (right).

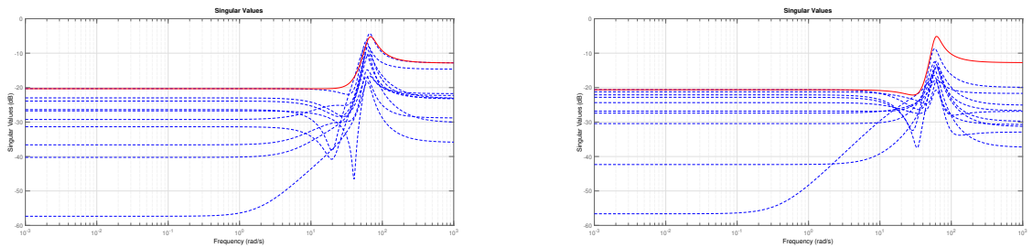

Figure 12: Order two, run one (left) and two (right).

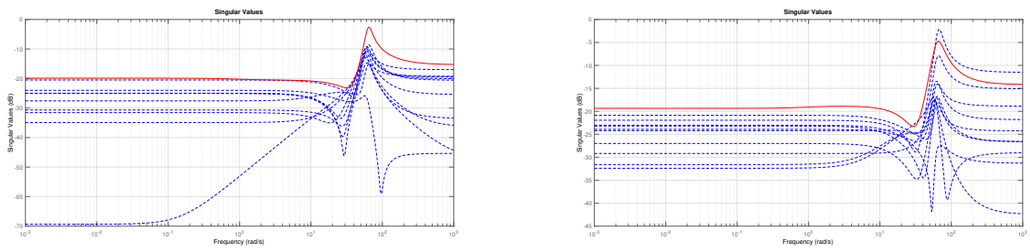

Figure 13: Order four, run one (left) and two (right).

We choose the fourth-order template as the best upper bound of the uncertainties since the first order does not reflect the behavior of the uncertainties and since the second order is a bit delayed regarding the peaks. Higher orders are not taken since their performance might be better, but their complexity would arise.

Small gain theorem

Now that an upper bound has been chosen, we verify that the small gain theorem is satisfied, both for the $\mathcal{H}_\infty$ and the PD controllers. The small gain theorem for output multiplicative is satisfied if the T sensitivity functions stay under $1/W_4$.

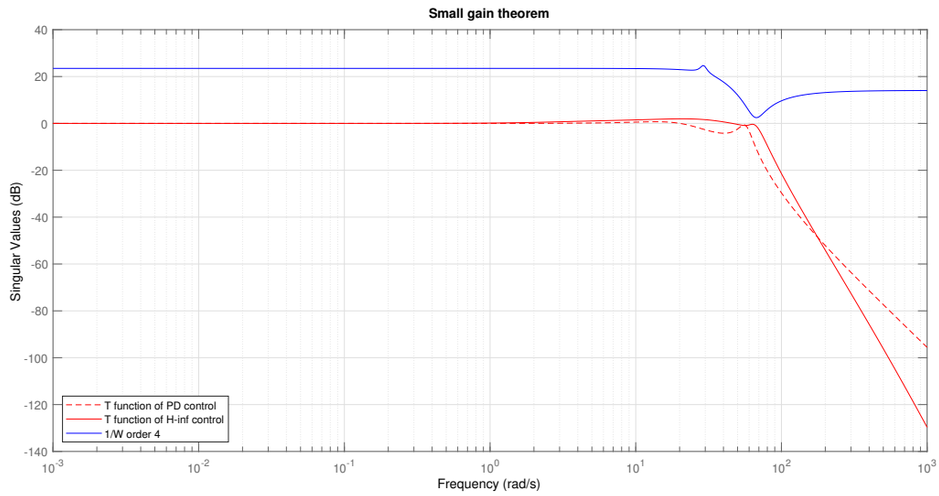

Figure 14: Frequency representation of the small gain theorem validation

We see that the small gain theorem is satisfied and the relative error between T and $1/W$ is suitable.

3 Chassis control: Roll and bounce

In this section, a half-car model is used, and we try to find a controller that allows an improvement of the passengers' comfort regarding the car's suspension.

3.1 System description

The system used in this section is described by a half-car model, which consists of the front axle of a car. The model is shown in Figure 15. In addition to the bounce moments, this model allows taking into account the vehicle roll moment.

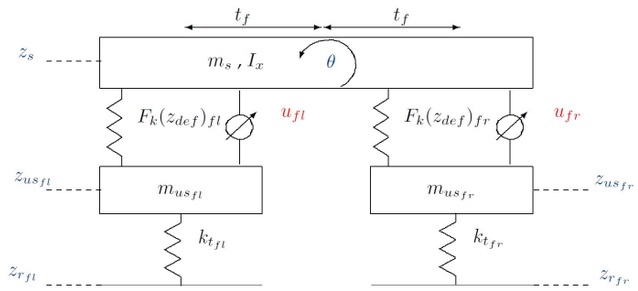

Figure 15: Half vehicle semi-active model.

The model is obtained by the combination of two suspension equations and the dynamical equation of the chassis. The model is given in a MATLAB file.
Passenger comfort is evaluated by the response of the sprung mass displacement and the roll angle from the road signal in low frequencies in the range of $1Hz$ to $10Hz$.

3.2 Controller design

To improve passenger comfort, the weighting functions W_{zs} and W_{roll} used in the general control configuration have to be appropriately chosen. W_{zs} is linked to the vertical movement of the chassis, whereas W_{roll} is linked to the rolling, which makes W_{zs} and W_{roll} relevant concerning the comfort.
In an open-loop configuration, the systems frequency response shows two peaks, the first one around $1Hz$ and a second one at approximately $10Hz$. The objective is to lower the first peak since it is the chassis one (as for the 1/4 model). However, the second peak must not be lowered since it is from the wheel motions.
First, the weighting functions W_{zr1} and W_{zr2} are chosen such that they represent a bump of 10mm. Figures 16 and 17 show the open-loop and closed-loop responses for z_s/z_r and θ/z_r.

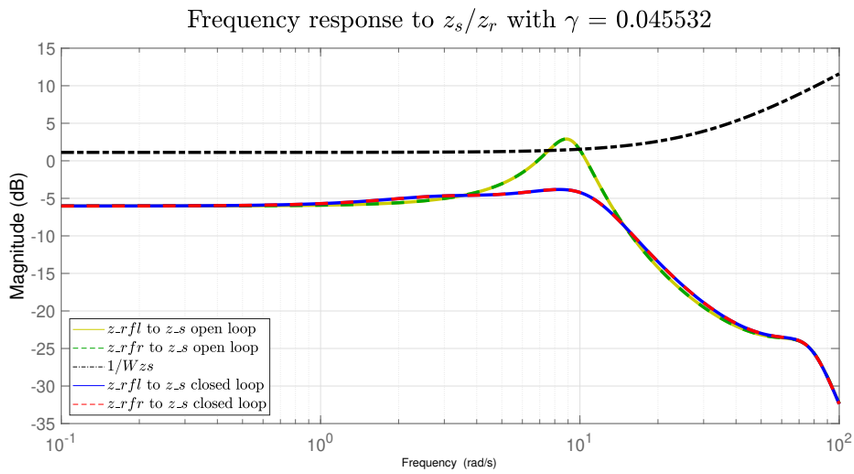

Figure 16: Frequency response and weighting function for z_s

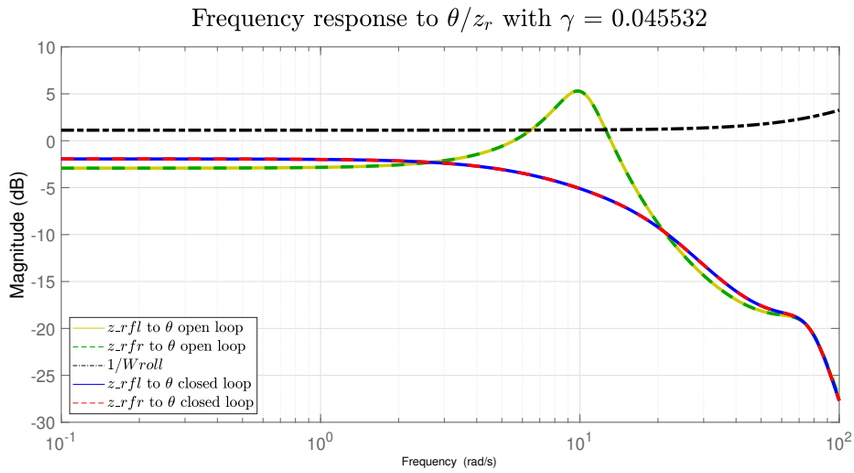

Figure 17: Frequency response and weighting function for θ

The parameters of the weighting functions are chosen as follows. For W_{zs}, the filter's cutoff frequency is chosen as $1Hz$ as a first trial. Since the cutoff frequency is set too low to considerably impact the peak at around $1Hz$, it is increased to $5Hz$. Then, in order not to attenuate the second peak, the second cutoff frequency is set to $20Hz$.
Furthermore, a gain of 4 is chosen in order to lower the weighting function and thus the peak of the frequency response at $1Hz$.
The weighting function results are shown in Figures 16 and 17, as a black dashed line. Besides, the graphs show the closed-loop system response in blue/red for the left/right wheel. As expected, the peak at $1Hz$ has been considerably attenuated in both cases, the vertical movement and the roll movement.

3.3 Validation using simulation

Time-domain simulations are then performed to complete the evaluation. For instance, this simulation considers a $10mm$ bump under the right wheel (from $5s$ to $8s$) and a $10mm$ bump under the left wheel (from $1s$ to $3s$). The simulation also enables us to test the controller with and without disturbances.

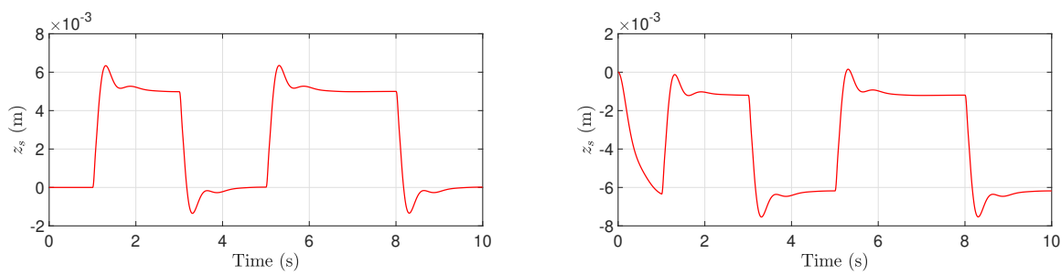

Figure 18: z_s without disturbances (left) and with disturbances (right).

With or without disturbances, we observe that the controller is performing well at dampening the bump in small oscillations which quickly stop after less than a second.

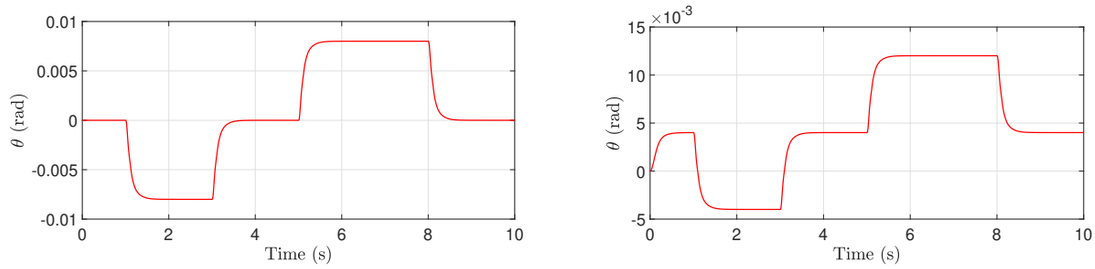

Figure 19: θ without disturbances (left) and with disturbances (right).

Additionally, the roll of the car is performing well for a bump on the left side and then a bump of the right side, with or without disturbances.

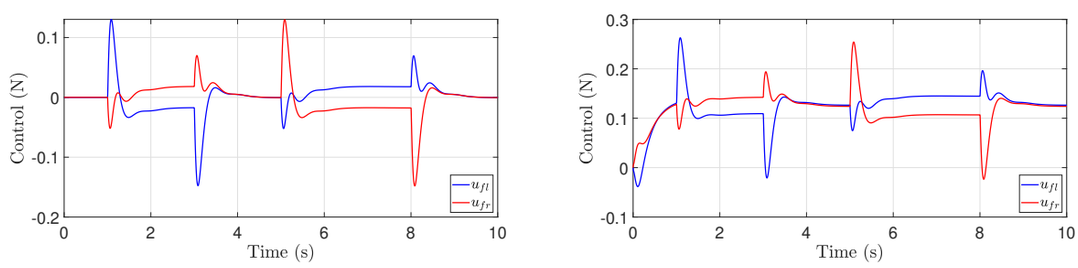

Figure 20: u without disturbances (left) and with disturbances (right).

Also, the control input is kept at a small value and the variations stop quickly (the control actuators have limited forces). Lastly, by changing the weighting functions W_u to 0.14, we also succeed in keeping the suspension within its bounds: $z_{def} \in [-0.09, 0.05]m$ as shown below:

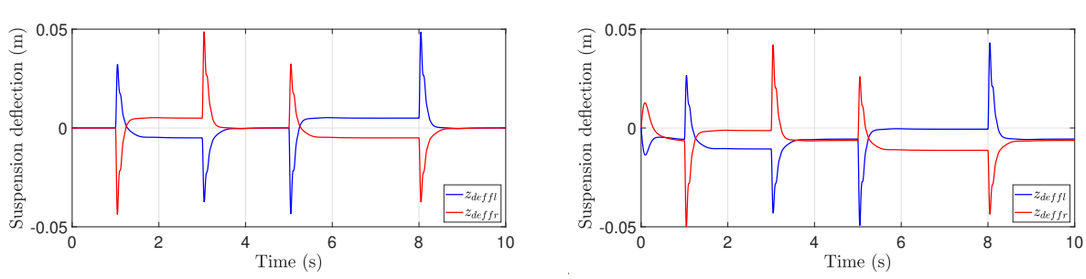

Figure 21: z_{def} without disturbances (left) and with disturbances (right).

Time-domain simulations prove that our choice of weighting functions provides a satisfactory solution according to the performance specifications, namely the comfort improvement evaluated through the sprung mass displacement $z_s(t)$ and of the roll angle $\theta(t)$ from the road signal $z_r(t)$ in low frequencies ($[1-10]Hz$).

4 Conclusion

After this lab, we understand better the robust approach in control. We now know the importance of analyzing sensitivity functions regarding a set of specifications, which is intuitive. We also know how to propose a template and to modify it depending on different tests. We also study the robustness of our controller and learn how to satisfy the small gain theorem. Furthermore, this lab shows us the importance of weighting functions in a practical and interesting example.